Functional connectivity of insular efferences

Talal Almashaikhi, Sylvain Rheims, Julien Jung, Karine Ostrowsky-Coste, Alexandra Montavont, Julitta de Bellescize, Alexis Arzimanoglou, Pascale Keo Kosal, Marc Guénot, Olivier Bertrand, et al.

◆ Human Brain Mapping 35:5279–5294 (2014) ◆

Functional Connectivity of Insular Efferences

Talal Almashaikhi,[1,2,3] Sylvain Rheims,[1,4] Julien Jung,[2] Karine Ostrowsky-Coste,[2] Alexandra Montavont,[1,2,4] Julitta De Bellescize,[2] Alexis Arzimanoglou,[1,2] Pascale Keo Kosal,[2] Marc Guénot,[5] Olivier Bertrand,[6] and Philippe Ryvlin[1,2,3,4]*

[1]*TIGER, Lyon's Neuroscience Research Centre, INSERM U1028, CNRS 5292, UCB Lyon 1, Lyon, France*
[2]*Department of Sleep, Epilepsy and Pediatric Clinical Neurophysiology, Hospices Civils de Lyon, Lyon, France*
[3]*Department of Clinical Physiology, Neurophysiology Division, Sultan Qaboos University Hospital, Muscat, Oman*
[4]*Department of Functional Neurology and Epileptology, Hospices Civils de Lyon, Lyon, France*
[5]*Department of Functional Neurosurgery, Hospices Civils de Lyon, Lyon, France*
[6]*DYCOG, Lyon's Neuroscience Research Centre, INSERM U1028, CNRS 5292, UCB Lyon 1, Lyon, France*

Abstract: *Objectives:* The aim of our study was to explore the functional connectivity between the insula and other cortical regions, in human, using cortico-cortical evoked potentials (CCEPs) *Experimental design:* We performed intra-cerebral electrical stimulation in eleven patients with refractory epilepsy investigated with depth electrodes, including 39 targeting the insula. Electrical stimulation consisted of two series of 20 pulses of 1-ms duration, 0.2-Hz frequency, and 1-mA intensity delivered at each of the 39 insular bipoles. Rates of connectivity were reported whenever a noninsular cortical region was tested by at least ten stimulating/recording electrode pairs in three or more patients *Results:* Significant CCEPs were elicited in 193 of the 578 (33%) tested connections, with an average latency of 33 ± 5 ms. The highest connectivity rates were observed with the nearby perisylvian structures (59%), followed by the pericentral cortex (38%), the temporal neocortex (28%), the lateral parietal cortex (26%), the orbitofrontal cortex (25%), the mesial temporal structures (24%), the dorsolateral frontal cortex (15%), the temporal pole (14%), and the mesial parietal cortex (11%). No connectivity was detected in the mesial frontal cortex or cingulate gyrus. The pattern of connectivity also differed between the five insular gyri, with greater connectivity rate for the posterior short gyrus (49%), than for the middle short (29%), and two long gyri (28 and 33%) *Conclusion:* The human insula is characterized by a rich and complex connectivity that varies as a function of the insular gyrus and appears to partly differ from the efferences described in nonhuman primates. *Hum Brain Mapp 35:5279–5294, 2014.*

Key words: insular; functional connectivity; intra-cranial electrical stimulation; evoked potential; human

Additional Supporting Information may be found in the online version of this article.

*Correspondence to: Pr Philippe Ryvlin, Unité 301, Hôpital Neurologique, 59 bd Pinel, 69003 Lyon, France.
E-mail: ryvlin@cermep.fr

Received for publication 3 September 2013; Accepted 6 May 2014.

DOI: 10.1002/hbm.22549
Published online 19 May 2014 in Wiley Online Library (wileyonlinelibrary.com).

INTRODUCTION

Our knowledge of insular connectivity in primates primarily derives from macaque tracer injection data and human neuroimaging studies. In macaques, the insula has reciprocal connections with nearby medial temporal, temporopolar and orbitofrontal cortex, as well as with the anterior cingulate gyrus and lateral prefrontal areas [Mesulam and Mufson, 1982; Mufson and Mesulam, 1982]. Differences exist in the topographic distribution of projections from and into the sub regions of the macaque's insula, whereby its anterior aspect is extensively connected with the amygdala, orbitofrontal cortex, anterior cingulate gyrus, temporal pole, and entorhinal cortex, while its posterior part is preferentially connected to the premotor cortex, first and second somatosensory cortices, superior temporal sulcus, and posterior cingulate gyrus [Augustine, 1986; Mesulam and Mufson, 1985]. This organization is consistent with the anterior to posterior cytoarchitectonic gradient of the insula, progressively shifting from agranular, to dysgranular and granular cortices [Mesulam and Mufson, 1982].

Similarly, resting state functional connectivity measures in human have identified an anterior and a posterior insular functional network [Cauda et al., 2011]. The former links the anterior insula to the middle and inferior temporal cortex as well as to the anterior cingulate gyrus, and is responsible for emotional salience and cognitive control. The posterior network links the middle-posterior insula to premotor, sensorimotor, supplementary motor and middle-posterior cingulate cortices, and primarily supports verbal, auditory, and motor processing. Probabilistic tractography and structural connectivity mapping are also in agreement with this bipartition of the human insula [Cloutman et al., 2011] and rostrocaudal trajectory of connectivity reflecting cytoarchitectony [Cerliani et al., 2011].

However, the above findings do not provide details about the functionality and latency of the identified connections. Such information can be obtained by generating cortico-cortical evoked potentials (CCEPs) through low-frequency electrical brain stimulation (EBS) in patients undergoing intracerebral EEG investigation (icEEG) for refractory partial epilepsy [Catenoix et al., 2005, 2011]. Investigating the insula is of particular interest in patients with epilepsy, since this region might be the site of seizure onset, mimicking temporal or frontal lobe epilepsy through its propagation pathways [Ryvlin, 2006; Ryvlin and Kahane, 2005; Ryvlin et al., 2006a]. So far, however, EBS was primarily applied to the insula using high frequency stimulation to trigger signs or symptoms informing on its functional role, but not on its connectivity [Afif et al., 2010a,b; Ostrowsky et al., 2000, 2002; Pugnaghi et al., 2011; Stephani et al., 2011]. Recently, we have examined the intra-insular connectivity using low-frequency EBS, and described reciprocal connections between most of the five insular gyri [Almashaikhi et al., 2013]. In the current study we used the same technique to examine the functional efferences of the human insula.

MATERIALS AND METHODS

Patients

The study included eleven patients with drug-resistant partial epilepsy undergoing icEEG as part of presurgical assessment of their epilepsy, including the ten patients previously reported in a CCEP study of intrainsular connectivity [Almashaiki et al., in press]. All patients had a morphologically normal insula on MRI. Extra insular cortical lesions were observed in four patients, including a left temporo-frontal cortical dysplasia, a right frontal cortical dysplasia, a right parietal porencephalic cyst, and two tubers (right temporal pole and left frontal) in a patient with a minor form of tuberous sclerosis. Another four patients demonstrated hippocampal atrophy or malrotation, which were bilateral in half of them. All patients and caregivers gave their informed consent to participate to this study.

Stereotactic Implantation of Depth Electrodes

IcEEG was performed according to the technique described by Talairach and Bancaud [1973], a procedure used routinely in our department [Guenot et al., 2001]. The brain regions to be investigated were determined for each patient, based on individual presurgical data, and most likely origin of seizure onset. Electrodes were implanted perpendicular to the mid-sagittal plane with the patient's head fixed in the Talairach's stereotactic frame. Eleven to sixteen semirigid intracerebral electrodes were implanted per patient, including at least one which targeted the insula ipsilateral to the putative ictal onset zone in all patients. Two patients had bilateral implantation. Each electrode was 0.8 mm in diameter and included 5, 12, or 15 contacts 2 mm in length, 1.5 mm apart (Dixi, Besançon, France), depending on the target region.

A total of 39 insular electrodes were placed in the eleven patients, including ten in the right insula and 29 in the left insula. The median number of insular electrodes per patient was 3 (range 1–6). Three electrodes explored the anterior short gyrus (ASG), four the middle short gyrus (MSG), seven the posterior short gyrus (PSG), 11 the anterior long gyrus (ALG), and 14 the posterior long gyrus (PLG). Thanks to the orthogonal implantation, the two deepest leads of each insular electrodes were always located within the same insular gyrus. Apart from these 39 insular electrodes, 5–13 electrodes were implanted in each patient (median = 10) (see Supporting Information Table I). A single electrode could sample different structures along its course in the cortex, while the same brain region could be sampled by several electrodes in the same patient. The investigated brain regions included the hippocampus

TABLE I. Epileptogenic zone as determined by SEEG

Patient no.	SOZ determined by SEEG	No. of electrodes	Lobes investigated
1	Right mesial temporal	13	Front. (M, L), Temp. (M,L), Occ.
2	Bilateral hippocampi	14	Front. (M, L), Pariet. (M,L), Temp. (M,L),
3	Left insula	11	Front. (M, L), Pariet. (M, L), Temp. (L),
4	Left third frontal gyrus	12	Front. (M, L), Pariet. (L), Temp. (M,L),
5	Left orbitofrontal	15	Front. (M, L), Temp. (M,L),
6	Right temporal pole	14	Front. (M, L), Pariet. (M,L), Temp. (M,L),
7	Left mesial temporal	11	Front. (M, L), Pariet. (L), Temp. (M,L),
8	Right lateral parietal	13	Front. (M, L), Pariet. (M,L), Temp. (L), Occ.
9	Left frontal mesial	16	Front. (M, L), Pariet. (M,L)
10	Right lateral temporal	12	Front. (M, L), Pariet. (L), Temp. (L),
11	Right post central gyrus	12	Front. (M, L), Pariet. (M,L)

($n = 12$ electrodes), the entorhinal cortex ($n = 3$ electrodes), the amygdala ($n = 3$ electrodes), the parahippocampus ($n = 2$ electrodes), the temporal neocortex ($n = 56$ electrodes), the orbitofrontal cortex ($n = 8$ electrodes), the mesial frontal cortex ($n = 10$ electrodes), the dorsolateral frontal cortex ($n = 26$ electrodes), the frontal operculum ($n = 20$ electrodes), the parietal operculum ($n = 8$ electrodes), the parietal lobe ($n = 19$ electrodes), and the occipital lobe ($n = 3$ electrodes).

The exact location of each electrode and recording lead was evaluated on a postimplantation MRI. In all but one patient (#7), we spatially normalized this MRI onto the MNI template and calculated MNI coordinates of each recording and stimulating leads (see Supporting Information Table II).

Seizure Onset Zone

The seizure onset zone (SOZ) was defined by icEEG recordings as the epileptogenic cortex which shows the first clear ictal EEG change and needs to be resected to produce seizure freedom (Table I). Areas of secondary spread were also identified on icEEG recordings as the cortical regions recruited during the course of the ictal discharge but which were not involved at seizure onset.

TABLE II. Divergence of insular efferences

Insular gyrus	No. of stimulated bipoles	No. of brain regions showing CCEP per stimulated bipole		
		Median	Mean ± SD	Range
ASG	3	5	5 ± 3	2–8
MSG	4	2.5	2.8 ± 2.5	0–6
PSG	7	4	3.9 ± 1.3	1–5
ALG	11	3	3.5 ± 1.8	1–6
PLG	14	3.5	3.5 ± 1.7	1–6
Total	39	4	3.6 ± 1.8	0–8

The insula was part of the SOZ in one patient (#3) and included in the area of secondary spread in two others (#2, #7). In patient #3, seizures originated within the left insula (PSG, ALG, and PLG) and then spread to the ipsilateral inferior frontal gyrus and superior temporal gyrus. In patients #2 and #7, seizures initiated within the mesial temporal structures and then spread to the ipsilateral insula (PSG, ALG, and PLG for patient #2; PLG for patient #7).

The SOZ of the eight other patients was frontal in three (#4, #5, #9), parietal in two (#8, #11), and temporal in three (one mesial temporal (#1), one temporo-polar (#6), and one lateral temporal (#10)).

For further analysis, recorded contacts were divided into those located in the epileptogenic zone (epileptic contacts), and those located elsewhere (nonepileptic contacts).

Brain Stimulation and CCEP Recordings

EBS is routinely and systematically performed in our patients undergoing icEEG as part of the clinical investigation to assess the epileptogenicity and functionality of the implanted brain regions. Stimulations at 50 and 1 Hz aim at triggering ictal signs, epileptic discharges, or full-blown seizures [Kahane et al., 1993, 2004; Munari et al., 1993], whereas 0.2 Hz are used to trigger abnormal cortical evoked responses (i.e., delayed to more than 100 ms or repetitive) suggestive of an underlying epileptogenic cortex [Valentin et al., 2002, 2005a,b; van't Klooster et al., 2011]. In addition to their clinical utility, 0.2-Hz stimulations also allow to measure physiological early responses, referred to as cortico-cortical evoked potentials (CCEPs) in this study, and reflecting brain connectivity [Brazier, 1964; Buser and Bancaud, 1983; Buser et al., 1992; Catenoix et al., 2005, 2011; Lacruz et al., 2007; Matsumoto et al., 2004, 2007; Rosenberg et al., 2009; Rutecki et al., 1989; Wilson et al., 1990]. We performed 0.2-Hz stimulations at least 4 days following electrodes implantation, once the patient has fully recovered from the surgical procedure.

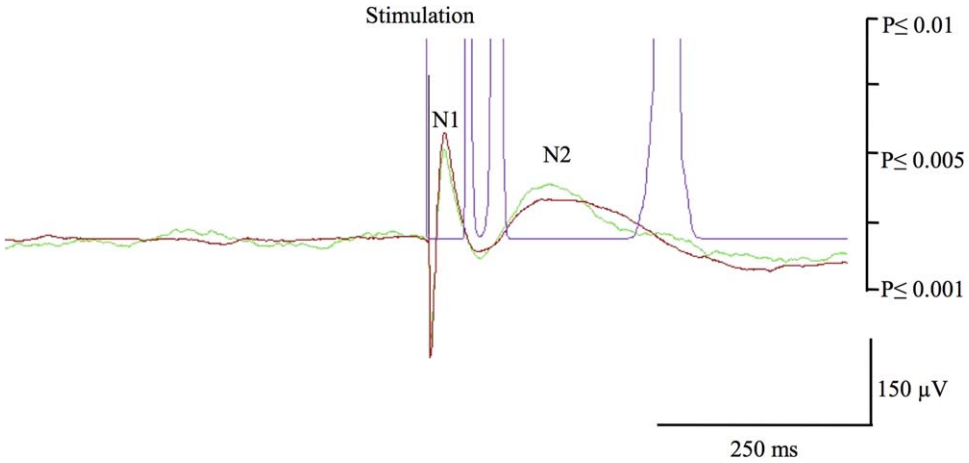

Figure 1.

Illustration of a cortico-cortical evoked potential in response to insular stimulation. Negative polarity is upward. The green and red color superimposed curves are the average of two consecutive 20-trials showing similar N1 and N2 peaks. The purple curve represents the *P* statistic which value is <0.001 threshold (i.e., significant response) when reaching the abscissa.

We used bipolar stimulation of adjacent contacts from the same electrode, known to deliver current within 5 mm around the stimulated bipole [Nathan et al., 1993]. Electrical stimulation was delivered using a current-regulated neurostimulator (Micromed, Treviso, Italy), with parameters ensuring patient safety and effective generation of CCEPs [Catenoix et al., 2005, 2011; Gordon et al., 1990]. We used monophasic pulse of 1 ms width and 1-mA intensity resulting in an electrical charge of 1 μC. The latter was delivered over a contact surface of 0.05 cm^2 (0.8 mm diameter × 2 mm length × π), resulting in a total charge density of 20 $\mu C/cm^2$/phase, thus significantly lower than the maximum safe value of 60 $\mu C/cm^2$/phase [Gordon et al., 1990]. Two consecutive series of 20 pulses were delivered at each pair of contacts. Intracerebral recordings were performed using a video-EEG monitoring system (Micromed, Treviso, Italy) that allowed to simultaneously recording 128 contacts at a sampling rate of 1,024 Hz.

Data Analysis

EEG data were analyzed with the software package for electrophysiological analysis (ELAN-pack) developed at the DYCOG laboratory of Lyon Neuroscience Research Centre (CRNL, Lyon, France) [Aguera et al., 2011]. We first performed an automatic detection of the pulse artifact generated on the stimulated contacts, and systematically verified the accuracy of the generated marker. Thanks to the very reproducible shape and amplitude of artifacts, as well as the associated high signal to noise ratio, this procedure did not suffer from false positive or negative detection. We used the stimulation marker for averaging each block of 20 consecutive pulse stimulations, and then calculated grand averages from the two blocks. Both visual and statistical analyses were used to conclude on the presence of significant CCEPs over each recording contact. CCEPs were first selected on the basis of visual analysis if detected and found comparable in each of the two consecutive series. Statistical analysis of the selected CCEPs was then performed using the non-parametric statistical function of ELAN-pack for single trails (Wilcoxon test), with significance set at $P < 0.001$. In brief, this statistical analysis used a sliding window of 5-ms duration to compare each consecutive periods of the post-stimulation period to the 1,000 ms prestimulation baseline, providing a curve, superimposed on the CCEP, illustrating the *P* value associated with each component of the CCEP. The first 10-ms post-stimulation were not evaluated due to the presence of residual stimulation-induced artifact. CCEPs were considered significant when they reached the statistical threshold of $P \leq 0.001$. Most CCEPs are characterized by two peaks refered to as N1 and N2 (see Fig. 1), while a minority will only display a single peak [Almashaikhi et al., 2013; Matsumoto et al., 2004]. In accordance with previous studies in the field, we calculated the latency of the first peak (N1) of each significant potential on the grand average of the two series.

For each stimulated insular anatomical region, we analyzed the number of noninsular contacts showing significant CCEPs, and the latency of the earliest detected peak. This was done for epileptic and nonepileptic contacts separately. CCEPs were divided into short-distance connections, corresponding to those observed between the insula and the overlying perisylvian cortex (i.e., frontal, temporal, and parietal operculum), and long-distance connections for all other insular connections. For each identified insular efferent region, we searched for reciprocal connection by

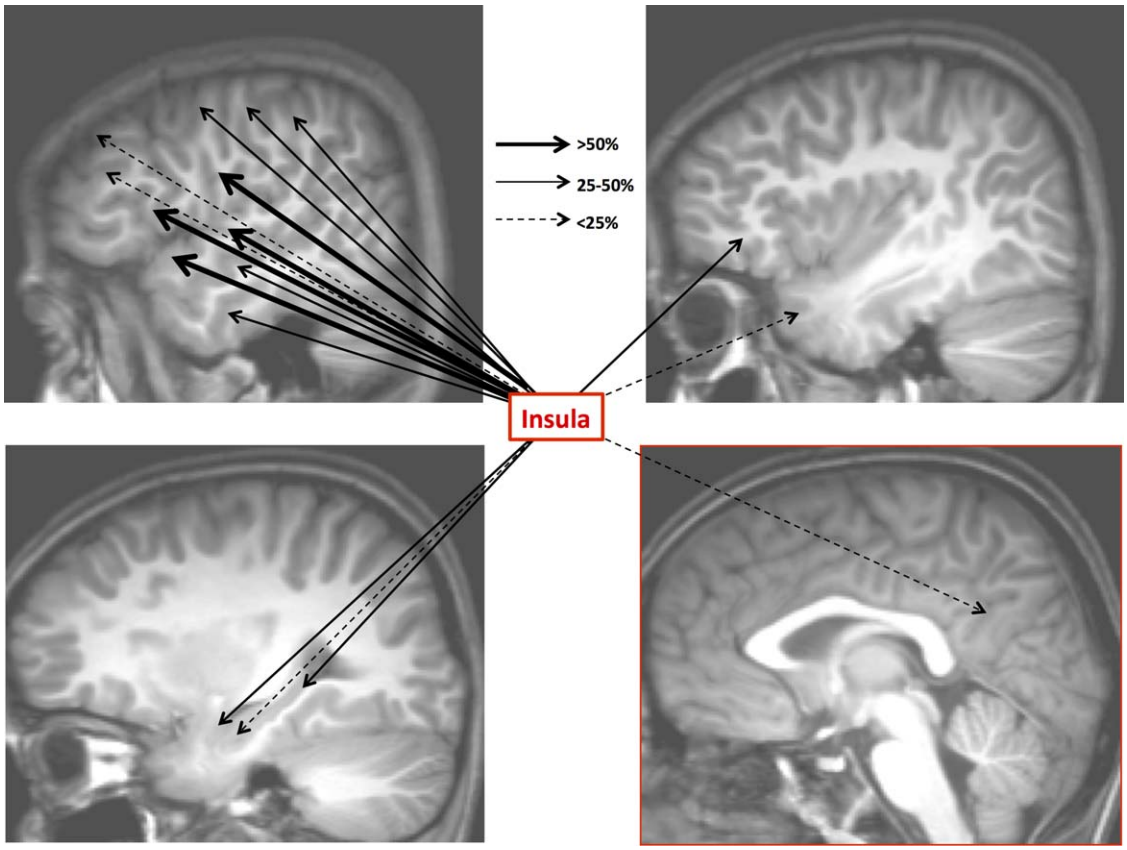

Figure 2.

Overall connectivity pattern of the insula: Upper left: Temporal neocortex, dorso-lateral frontal cortex, fronto-parietal operculum, temporo-parietal junction; Upper right: Insula, temporal pole, frontal pole and the fronto-orbital cortex; Lower left: mesio-temporal structures; Lower right: medial frontal, parietal and occipital cortices, cingulate gyrus. Thick plain black arrows: insular efferences with a connectivity rate $>$50%. Thin plain grey arrows: insular efferences with a connectivity rate $>$25% and $\leq$50%. Dashed black arrows: insular efferences with a connectivity rate $\leq$25%. [Color figure can be viewed in the online issue, which is available at wileyonlinelibrary.com.]

analyzing insular CCEPs elicited by stimulating this efferent region. These analyses were performed at the gyral level, considering the three short (ASG, MSG, and PSG) and two long gyri (ALG and PLG) as five distinct anatomical regions. The reason for choosing this segmentation were the following: (i) different functional parcellation of the insula have been proposed, considering either two, three of four distinct sub regions, making it difficult to rely on an objective and uniform functional framework; (ii) conversely, the division of the insula into its five gyri allows avoiding any ambiguity and an easy reconstruction of findings into the various functional parcellation previously identified; and (iii) gyral findings can be directly used for better understanding the propagation of epileptic discharges involving the insula, given that implantation of depth electrodes in patients undergoing SEEG is currently based on the identification of anatomical gyri, rather than functional regions.

Once a nonepileptic noninsular contact showed significant CCEPs after an insular stimulation in at least one patient, it was considered that the two regions were connected. Given the cortical sampling variability across patients, we could not determine whether the absence of visualized CCEP between a specific insular region and a specific extrainsular cortical region reflected the absence of functional connection or the limited sampling within the insular cortex and/or the noninsular region. In this context, connectivity was analyzed using the following empirical rules: (i) when a connection between an insular gyrus and a noninsular region was sampled by $\geq$10 stimulation/recording electrode pairs in at least three different patients: a rate of connectivity was calculated, the presence of at least one significant CCEP in a nonepileptic noninsular region was considered as reflecting a functional connectivity between the two tested structures, while the lack of CCEP in all tested connections was considered as

TABLE III. Connectivity pattern of the insula

		Insular gyri					Entire insula	Reciprocity
		ASG	MSG	PSG	ALG	PLG		
Amygdala		0/1	0/1	1/2; 28 ms	2/3; 25 ± 3 ms	1/4; 30 ms	4/11 (36%) 28 ± 3 ms	100%
Hippoc.	Ant	2/2; 34 ± 22 ms	0/2	0/4	1/6; 40 ± 5 ms	1/9; 37 ms	4/23 (17%) 37 ± 3 ms	100%
	Post	1/1; 32 ms	1/2; 29 ms		1/4; 45 ms	1/5; 35 ms	4/12 (33%) 35 ± 7 ms	100%
Entorhinal cortex			0/1		1/3; 32 ms	1/4; 37 ms	2/8; 35 ± 4 ms	100%
Temporal pole		1/2; 49 ms	1/2; 36 ms	0/3	0/6	1/9; 32 ms	3/22 (14%) 39 ± 9 ms	100%
Parahippoc. gyrus				0/1	0/1	0/2	0/4	
Fusiform. gyrus					0/2	0/2	0/4	
Inf tempor. gyrus		1/1; 41 ms	1/2; 30 ms		3/7; 35 ± 13 ms	1/10 (10%) 31 ms	6/20 (30%) 34 ± 4 ms	83%
Mid tempor. gyrus		2/5; 30 ± 2 ms	0/5	4/9; 39 ± 2 ms	3/16 (19%) 50 ms	8/22 (36%) 25 ± 2 ms	17/57 (30%) 36 ± 1 ms	94%
Sup tempor. gyrus (Temporal operculum)	Ant	1/3; 37 ms	4/5; 32 ± 7 ms	8/12 (67%) 26 ± 6 ms	3/11 (27%) 35 ± 5 ms	14/17 (82%) 25 ± 2 ms	30/48 (63%) 31 ± 5 ms	87%
	Post	1/2; 30 ms	1/3; 20 ms	4/6; 33 ± 14 ms	4/10 (40%) 26 ± 3 ms	10/15 (67%) 28 ± 3 ms	20/36 (56%) 27 ± 5 ms	95%
Orbito-frontal		3/3; 33 ± 5 ms	0/3	1/3; 40 ms	1/7; 40 ms	1/8; 65 ms	6/24 (25%) 44 ± 14 ms	100%
Frontal pole		0/1	0/2		0/2	0/1	0/6	
Inf frontal gyrus (front. operculum)		4/7; 28 ± 8 ms	8/12; (67%) 29 ± 4 ms	10/14 (71%) 29 ± 4 ms	11/19 (58%) 35 ± 5 ms	8/23 (35%) 26 ± 3 ms	41/75 (55%) 29 ± 3 ms	85%
Mid frontal gyrus		2/4; 35 ± 3 ms	0/6	2/2; 30 ± 1 ms	0/8	0/5	4/25 (16%) 32 ± 3 ms	100%
Sup frontal gyrus		0/3	0/3	1/3; 35 ms	1/5; 28 ms	1/2; 30 ms	3/16 (19%) 31 ± 4 ms	100%
Pre-SMA and SMA		0/1	0/2	0/4	0/6	0/4	0/17	
Cingulate gyrus	Ant	0/1	0/2	0/1	0/3	0/3	0/10	
	Mid	0/1	0/1		0/2		0/4	
	Post	0/1	0/1	0/1	0/3	0/3	0/9	
Precentral gyrus		0/3	1/4; 24 ms	3/5; 33 ms	6/10 (60%) 30 ± 7 ms	1/7; 24 ± 3 ms	11/29 (38%) 27 ± 5 ms	83%
Postcentral gyrus					2/6; 23 ± 2 ms	2/4; 25 ± 3 ms	4/10 (40%) 24 ± 1 ms	100%
Parietal operculum		0/3	2/3; 36 ± 11 ms	5/6; 27 ± 3 ms	6/8; 27 ± 2 ms	7/9; 26 ± 5 ms	20/29 (69%) 43 ± 27 ms	95%
Lateral parietal (sup and inf lobule)		0/2	0/3	2/8; 38 ± 2 ms	3/14 (21%) 28 ± 7 ms	6/16 (38%) 27 ± 3 ms	11/43 (26%) 30 ± 1 ms	92%
Mesial parietal		0/1	0/1		1/13; 22 ms	2/13; 24 ± 2 ms	3/28 (11%) 23 ± 1 ms	67%
Occipital lobe					0/3	0/5	0/8	
Total opercular regions		6/15 (40%)	15/23 (65%)	27/38 (71%)	24/48 (50%)	39/64 (61%)	111/188 (59%)	91%
Total other regions		12/33 (36%)	4/43 (9%)	14/46 (30%)	25/130 (21%)	27/138 (20%)	82/390 (21%)	94%
Total		18/48 (38%)	19/66 (29%)	41/84 (49%)	49/178 (28%)	66/202 (33%)	193/578 (33%) 33 ± 5 ms	93%
Reciprocity		100%	89%	95%	88%	89%		

For each tested connection, numerator corresponds to the number of significant CCEPs and denominator the number of connections tested for that region. Corresponding % are provided in brackets only for sites where at least ten connections were tested in three patients or more. Bottom number is the mean latency in ms ± SD (if ≥ 2 CCEPs recorded). Empty cells correspond to regions where no connection was tested. ASG, MSG and PSG (anterior, middle and posterior short gyri), ALG and PLG (anterior and posterior long gyri). CCEP: Cortico-cortical evoked potential, ASG, MSG and PSG (anterior, middle, and posterior short gyri), ALG and PLG (anterior and posterior long gyri).

reflecting the lack of functional connectivity between the two structures; (ii) when a connection between an insular gyrus and a noninsular region was sampled by <10 stimulation/recording electrode pairs or in less than three different patients: rate of connectivity was not calculated, the presence of at least one significant CCEP in a nonepileptic non insular region was still considered as reflecting a functional connectivity between the two tested structures, but no conclusion was drawn from the lack of CCEP in all tested connections.

The global connectivity rates of the five insular gyri were compared to each other using χ^2 statistic.

RESULTS

An overview of insular connectivity is shown in Figures 2–7 while detailed characteristics of CCEPs (presence, rate, latency, reciprocity) are provided in Table III.

A total of 578 electrode pairs were tested. Significant CCEPs were elicited in 193 of these 578 tested connections (TC) (33%). Recorded CCEPs typically corresponded to biphasic early responses, with a first negative peak (N1) occurring at an average ± SD latency of 33 ± 5 ms (range 24–44 ms), usually followed by a second negative peak (N2) (Fig. 1). Short-distance connections with the opercular regions had similar latencies to long-distance connections with other brain regions (33 ± 7 ms vs. 33 ± 6 ms). About 179 of these 193 connections were reciprocal (93%). Only one of the 32 interhemispheric TC in two patients (#2, #6) elicited a significant CCEP, specifically by stimulating the left MSG and recording from the right parietal operculum.

The morphology and latency of CCEPs triggered at each insular contact were comparable for the two stimulated bipoles part of the epileptogenic zone in patient #3 and for the 37 other stimulated bipoles, leading to pool all data for further results.

The highest occurrence of CCEPs was observed in the opercular regions (59%, $n = 188$ TC), with comparable rates for the temporal (60%, $n = 84$ TC), frontal (55%, $n = 75$ TC), and parietal operculum (69%, $n = 29$ TC) (Fig. 2). The overall insular connectivity was lower with the other brain regions (21%, $n = 390$ TC), including the pericentral cortex (pre- and postcentral gyri, 38%, $n = 39$ TC), nonopercular temporal neocortex (middle and inferior temporal gyri and fusiform gyrus, 28%, $n = 81$ TC), lateral parietal cortex (superior and inferior lobules, 26%, $n = 43$ TC), orbitofrontal cortex (25% $n = 24$ TC), mesial temporal structures (amygdala, hippocampus, entorhinal cortex, and parahippocampal gyrus, 24%, $n = 58$ TC), nonopercular lateral frontal cortex sSuperior and middle frontal gyri and frontal pole, 15%, $n = 47$ TC), temporal pole (14%, $n = 22$), and mesial parietal cortex (11%, $n = 28$ TC) (Fig. 2). Furthermore, no CCEP could be elicited in the mesial frontal cortex ($n = 31$ tested connections), including the SMA, pre-SMA, anterior and mid cingulate gyrus.

The connectivity rates of the five insular gyri showed significantly greater rate for the PSG (49%, $n = 84$ TC), than for the MSG (29%, $n = 66$ TC, $P < 0.025$), the ALG (28%, $n = 178$, $P < 0.01$), and the PLG (33%, $n = 202$, $P < 0.025$), but not than for the ASG (38%, $n = 48$ TC). No other significant difference was observed between ASG, MSG, ALG, and PLG. As detailed below, connectivity patterns varied across the five insular gyri, though this was not statistically tested due to too low sample size in many regions and unbalanced number of TC between insular gyri, and to avoid performing a meaningless number of statistical comparisons.

The number of distinct extra-insular brain regions showing CCEP in response to the stimulation of each individual insular bipole varied from 0 to 8, with a median of 4 and a mean ± SD of 3.6 ± 1.8 (see Table II and Fig. 3 for illustration). A single insular bipole located in the MSG was not associated with any detectable CCEP, while four other sites from the PSG, ALG, and PLG demonstrated CCEP in a single brain region. All other 34 insular bipoles generated CCEPs in at least two distinct brain regions. The rate of divergent connections was comparable between all five insular gyri (see Table II).

Anterior Short Gyrus (ASG)

A total of 48 connections were tested between the ASG and noninsular regions (Fig. 4, Table III). Functional connectivity was observed between the ASG and the hippocampus (all 3 TC) and orbitofrontal cortex (all 3 TC). CCEPs were also observed in the frontal operculum, temporal pole, temporal operculum, lateral temporal neocortex and dorsolateral frontal cortex. All connections were reciprocal.

Middle Short Gyrus (MSG)

A total of 66 connections were tested between the MSG and non-insular regions (Fig. 5, Table III). High rate connectivity was observed with the frontal operculum (67%, $n = 12$ TC). CCEPs were also recorded in the temporal and parietal operculum, as well with the hippocampus, the temporal pole and the primary motor cortex. Stimulation of the MSG did not elicit any CCEP in the dorsolateral frontal cortex ($n = 11$ TC), nor in the orbitofrontal cortex ($n = 3$ TC). Most connections were reciprocal (89%).

Posterior Short Gyrus (PSG)

A total of 84 connections were tested between the PSG and noninsular regions (Fig. 6, Table III). PSG was connected with the frontal (71%, $n = 14$ TC), and temporal operculum (67%, $n = 18$ TC). Connectivity was also observed with the parietal operculum, lateral temporal, frontal dorsolateral and lateral parietal cortex, precentral region, orbitofrontal cortex and amygdala, but not with the other temporolimbic regions ($n = 8$ TC). 95% of connections were reciprocal.

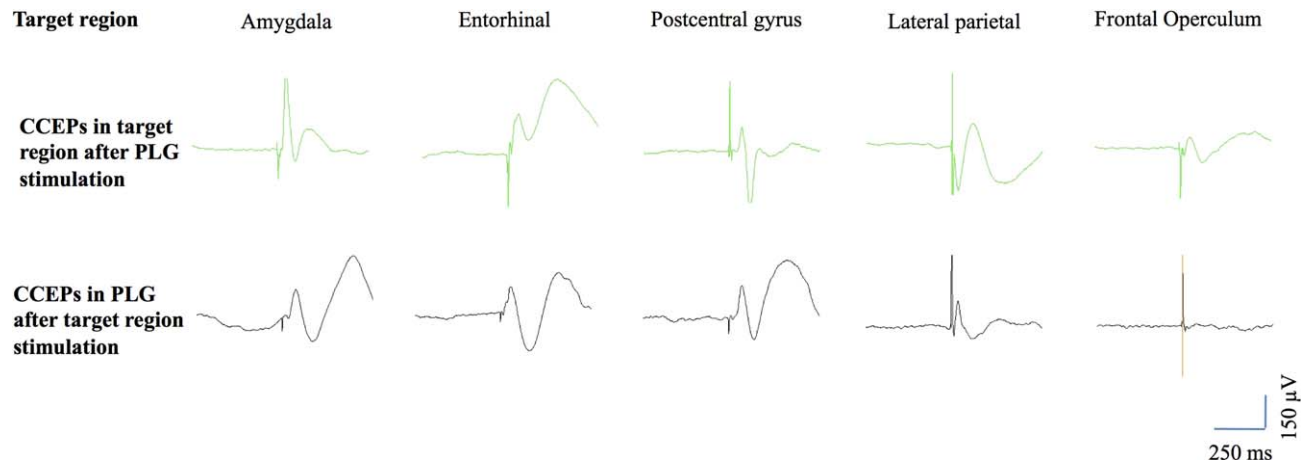

Figure 3.

Illustration of divergent and reciprocal cortico-cortical evoked potentials (CCEPs). The upper row shows CCEPs elicited by the stimulation of the posterior long gyrus (PLG) over five distinct brain regions. The lower row shows CCEPs generated in the PLG by stimulating the corresponding extra-insular brain region. Note that reciprocal connections are observed for the amygdala, entorhinal cortex, postcentral gyrus and lateral parietal cortex, but not for the frontal operculum. [Color figure can be viewed in the online issue, which is available at wileyonlinelibrary.com.]

Anterior Long Gyrus (ALG)

A total of 178 connections were tested between the ALG and non-insular regions (Fig. 7, Table III). Connections were again observed within the perisylvian region, but with a gradient showing higher rate of connectivity with the parietal (6 out of 8 TC) and frontal operculum (58%, $n = 19$ TC), than with the 1st temporal gyrus (33%, $n = 21$ TC). CCEPs were also elicited in the precentral gyrus (60%, $n = 10$ TC), lateral temporal neocortex (24%, $n = 25$ TC), lateral parietal cortex (21%, $n = 14$ TC), hippocampus (20%, $n = 10$ TC), as well as in the orbitofrontal cortex, superior frontal gyrus, postcentral gyrus, mesial parietal cortex, amygdala, and entorhinal cortex. No connection was observed with the temporal pole ($n = 6$ TC) and cingulate gyrus ($n = 8$ TC). 88% of connections were reciprocal.

Posterior Long Gyrus (PLG)

A total of 202 connections were tested between the PLG and noninsular regions (Fig. 8, Table III). PLG was connected to the perisylvian region, with higher connectivity rate with the temporal (75%, $n = 32$ TC) and parietal operculum (7 out of 9 TC), than with the frontal operculum (35%, $n = 23$ TC). CCEPs were also observed in the lateral parietal cortex (38%, $n = 16$ TC), lateral temporal cortex (26%, $n = 34$ TC), and hippocampus (14%, $n = 14$ TC), as well as in the temporal pole, amygdala, entorhinal cortex, orbitofrontal cortex, dorsolateral frontal cortex, pre- and postcentral gyri, and mesial parietal cortex. No connection was observed with the cingulate gyrus ($n = 6$ TC). 89% of connections were reciprocal.

Overall ASG showed the lowest connectivity rate with the perisylvian region (40%, $n = 15$ TC), but the highest rate with non opercular regions (36%, $n = 33$ TC), especially with the orbitofrontal cortex and the mesial temporal structures. MSG was characterized by very low connectivity rate with non opercular regions (9%, $n = 43$ TC). PSG had among the higher connectivity rates with both opercular (71%, $n = 38$ TC) and non opercular regions (30%, $n = 46$ TC), primarily with frontal and temporal lateral neocortex. ALG showed intermediate connectivity with both opercular (50%, $n = 48$ TC) and nonopercular regions (21%, $n = 117$ TC), with the latter concentrating on the mesial temporal structures, the precentral cortex, and to a lower extent, the parietal lobe. PLG also demonstrated intermediate connectivity rate with the perisylvian region (61%, $n = 64$ TC) and other brain regions (20%, $n = 138$ TC), in particular with lateral, and to a lesser degree mesial, parietal regions.

DISCUSSION

Tracer injections in macaques have delineated a complex and rich pattern of connectivity of the insula, which has been largely confirmed by human neuroimaging studies [Cauda et al., 2011; Cerliani et al., 2011; Cloutman et al., 2011; Deen et al., 2011; Mesulam and Mufson, 1982; Mufson and Mesulam, 1982]. However, details about the functionality, reciprocity and latency of the identified connections in human remain largely unknown. Our study

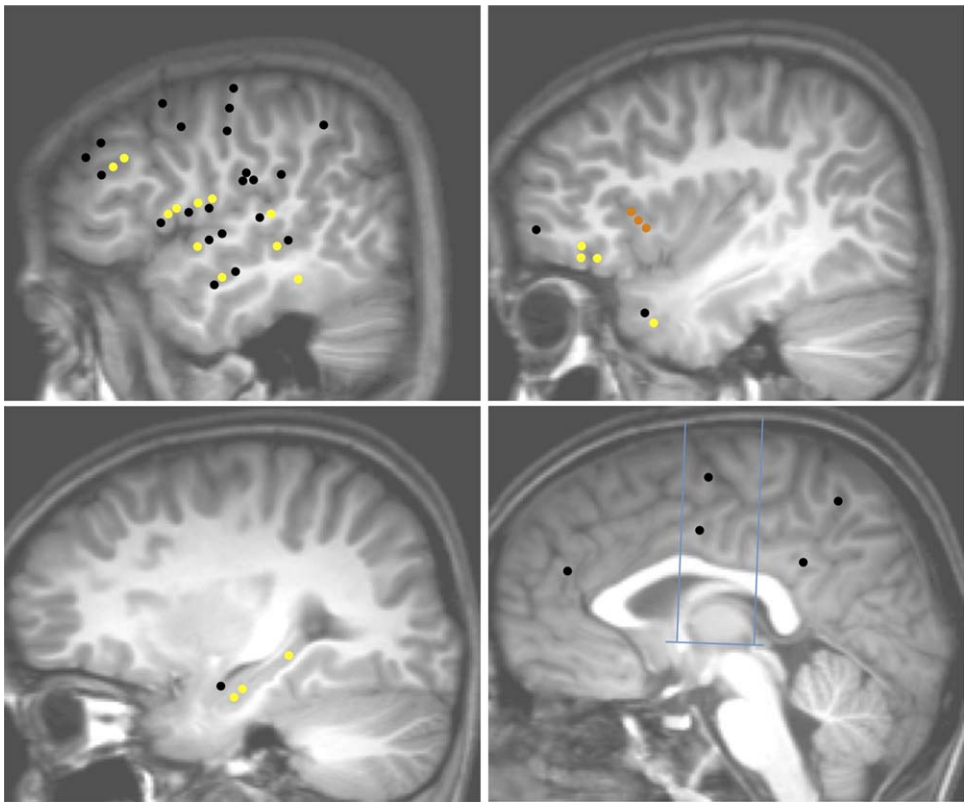

Figure 4.

ASG connectivity pattern: Upper left: Temporal neocortex, dorso-lateral frontal cortex, fronto-parietal operculum, temporo-parietal junction; Upper right: Insula, temporal pole, frontal pole and the fronto-orbital cortex; Lower left: mesio-temporal structures; Lower right: medial frontal, parietal, and occipital cortices, cingulate gyrus. Blue lines in the lower right figure indicate CA-CP axis and the orthogonal VCA and VCP axis. Yellow dots: connections demonstrating significant CCEPs; Black dots: connections without significant CCEP; Orange dots: ASG electrodes.

provides the first electrophysiological data on the efferent functional connectivity of the human Insula.

Using electrical brain stimulation and CCEP recordings, we observed dense functional efferent connectivity which main characteristics can be summarized as follows: (i) the highest connectivity rate (59%) was with the nearby perisylvian cortex (frontal, parietal, and temporal operculum), (ii) the highest long distance connectivity rates were with the pericentral region (41%), followed by the amygdala (36%), posterior hippocampus (33%), and lateral temporal neocortex (30%), (iii) most other testable connections associated with CCEPs had connectivity rates between 14 and 26%, and included the dorsolateral and orbital frontal cortex, the temporal pole, entorhinal cortex and anterior hippocampus, and the mesial and lateral parietal cortex, (iv) no connection was demonstrated with the cingulate gyrus (23 TC), mesial premotor cortex (17 TC), and fusiform and parahippocampal gyri apart from the entorhinal cortex (8 TC), occipital lobe (8 TC), and frontal pole (6 TC), v) most connections were reciprocal (93%), irrespective of the brain regions connected, (vi) the posterior short gyrus of the insula showed higher connectivity rate than most other insular gyri (except the anterior short) (vii) possible differences in the pattern of connectivity of the five insular gyri were also noted, but could not be statistically tested according to the sampling issue discussed below.

Indeed, several limitations of CCEPs interpretation deserve attention. Such studies are necessarily performed in patients with epilepsy, in whom the impact of seizures and interictal EEG discharges on brain connectivity remains a matter of debate [Meador and Hermann, 2010]. However, no difference between the early latency EPs (<100 ms) recorded from contacts included in the epileptic network and those recorded from nonepileptic tissue was observed in previous CCEP studies [Almashaikhi et al., 2013; Lacruz et al., 2007; Wilson et al., 1990], nor in this series. In addition, the insula was not part of the epileptogenic zone in 10 out of 11 patients, and was affected by the epileptic discharge during its

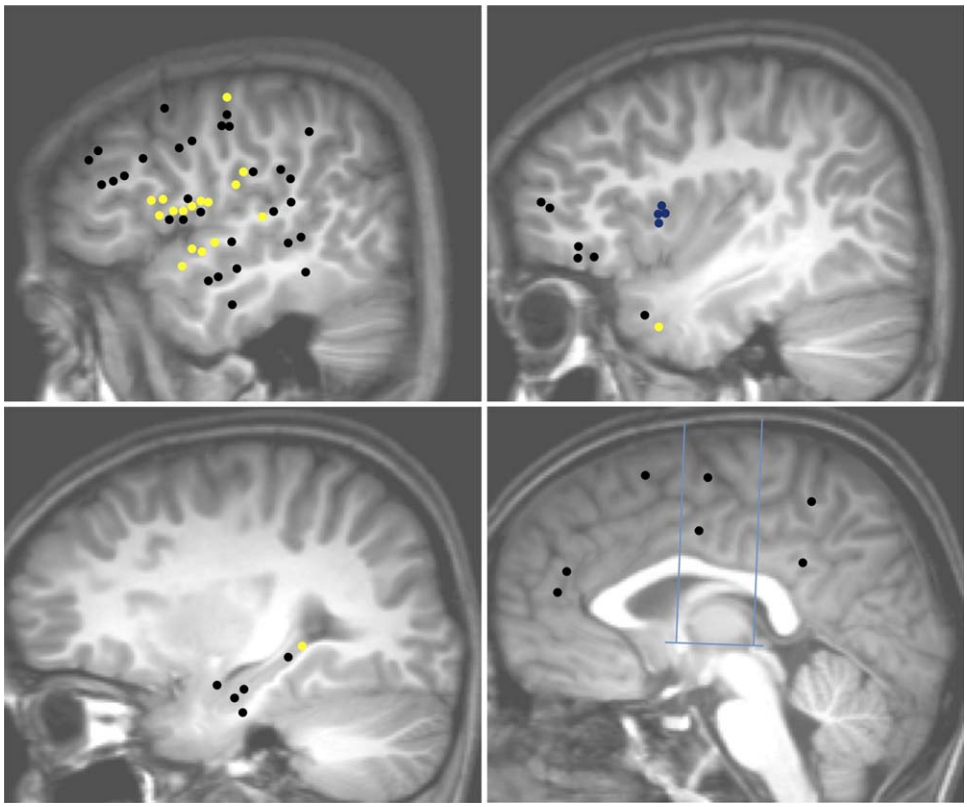

Figure 5.

MSG connectivity pattern: Upper left: Temporal neocortex, dorso-lateral frontal cortex, fronto-parietal operculum, temporo-parietal junction; Upper right: Insula, temporal pole, frontal pole and the fronto-orbital cortex; Lower left: mesio-temporal structures; Lower right: medial frontal, parietal and occipital cortices, cingulate gyrus. Blue lines in the lower right figure indicate CA-CP axis and the orthogonal VCA and VCP axis. Yellow dots: connections demonstrating significant CCEPs; Black dots: connections without significant CCEP; Blue dots: MSG electrodes.

propagation in only two other patients. Similarly, the majority of tested connections were not included within the epileptic network. Overall, we believe that our main findings are likely to apply to healthy individuals, though this cannot be firmly demonstrated. At least, the reported data are relevant to the understanding of propagation pathways of epileptic discharge originating in the insula. Other limitations are the small number of patients studied and the limited spatial sampling of intracerebral EEG investigations, both of which hamper any firm conclusion regarding lack of connection between the insula or one of its gyri and extra-insular cortical region. Indeed, the absence of visualized CCEP could either reflect the true absence of functional connection or lack of recording contact in the appropriate efferent target. Our criteria of testing a connection by at least ten electrode pairs in three or more patients to conclude on the presence or absence of functional connectivity might be too liberal, even though we did not observe one instance where a functional connection would be present in less than 10% of TC. A greater concern is the selective sampling of one or several sub regions within some of the cortical structures investigated, reflecting both the clinical practice and vascular constraint of SEEG. For instance, electrodes are not being placed in the anterior and inferior part of the insula, due to the vicinity of sylvian vessels. Another example is the anterior cingulate gyrus which pregenual aspect was the only portion targeted by depth electrodes, a limitation that might account for the lack of observed connectivity between the insula and this gyrus. In addition, the set of TC varied between each insular gyrus, which could account for part of the differences observed in connectivity rates. Finally, visual detection of CCEPs, hitherto used as the standard method to detect such potentials [Brazier, 1964; Buser and Bancaud, 1983; Buser et al., 1992; Catenoix et al., 2005, 2011; Lacruz et al., 2007; Rosenberg et al., 2009; Rutecki et al., 1989; Wilson et al., 1990], remains subjective and associated with an unknown rate of false positive or negative

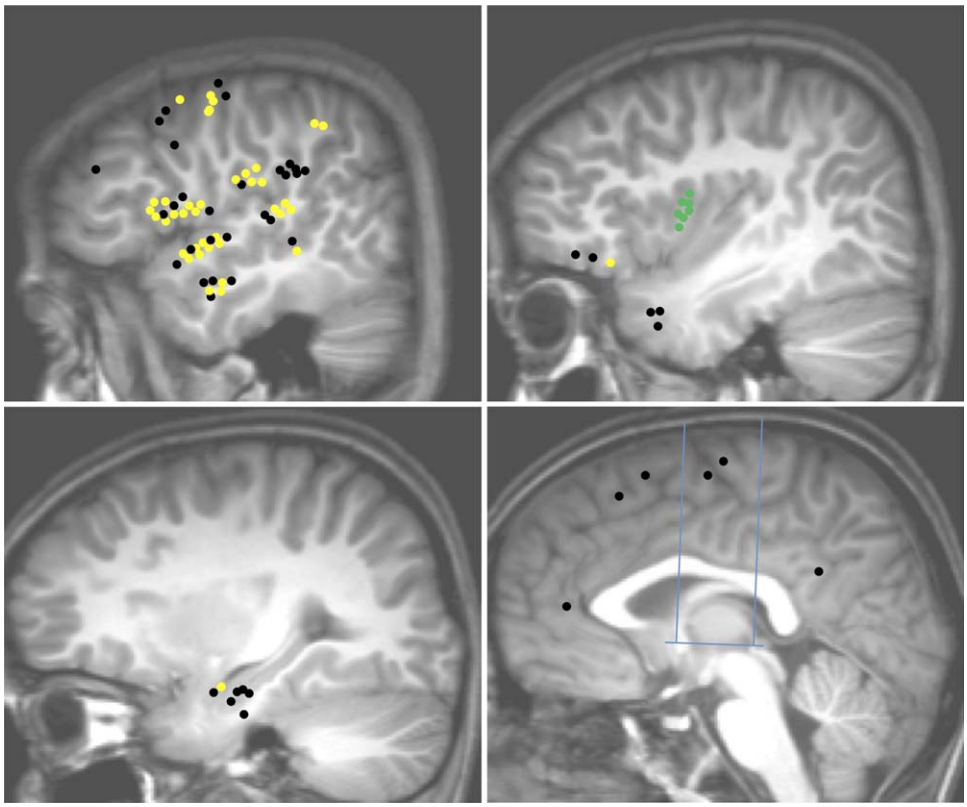

Figure 6.

PSG connectivity pattern: Upper left: Temporal neocortex, dorso-lateral frontal cortex, fronto-parietal operculum, temporo-parietal junction; Upper right: Insula, temporal pole, frontal pole and the fronto-orbital cortex; Lower left: mesio-temporal structures; Lower right: medial frontal, parietal and occipital cortices, cingulate gyrus. Blue lines in the lower right figure indicate CA-CP axis and the orthogonal VCA and VCP axis. Yellow dots: connections demonstrating significant CCEPs; Black dots: connections without significant CCEP; Green dots: PSG electrodes.

findings. We could reduce the risk of false positives by performing objective statistical tests, using an empirical threshold set at $P < 0.001$ without correction for multiple comparisons. Indeed, the high dependence between values recorded at each consecutive time points make standard bonferroni correction inappropriate in this setting.

Tracer injection studies in macaques as well as human neuroimaging studies have enabled to develop a framework whereby the connectivity between the insula and other brain regions has been divided into two complementary networks, one involving the anterior insula which plays a role in emotional aspects through connections with the amygdala, entorhinal cortex, orbitofrontal cortex, and anterior cingulate cortex, and another involving the posterior insula which is primarily involved in sensorimotor integration with predominant connections with the premotor cortex, first and second somatosensory cortices, superior temporal sulcus, and posterior cingulate gyrus [Cauda et al., 2011; Cerliani et al., 2011; Cloutman et al., 2011; Deen et al., 2011; Mesulam and Mufson, 1982; Mufson and Mesulam, 1982]. A parcellation of the human insula into three functionally distinct regions has also been proposed by several authors, based on cytoarchitectonic, DTI and functional MRI studies [Deen et al., 2011; Gallay et al., 2011; Jakab et al., 2011], while an activation-likelihood-estimation meta-analysis of 1,768 functional neuroimaging experiments concluded on the presence of four functionally distinct regions, mapping to the social-emotional, the sensorimotor, the olfacto-gustatory, and the cognitive network of the brain [Kurth et al., 2010].

According to the above studies, the anterior insula usually includes the first or first two short gyri of the insula, with or without the most anterior aspect of the long gyri. In monkeys, the anterior insula shows dense connections to limbic areas, including the amygdala, entorhinal cortex, temporal pole, orbitofrontal cortex, and anterior cingulate gyrus [Mesulam and Mufson, 1982, 1985; Mufson and Mesulam, 1982]. Functional imaging studies in human showed that the anterior insula is most strongly correlated

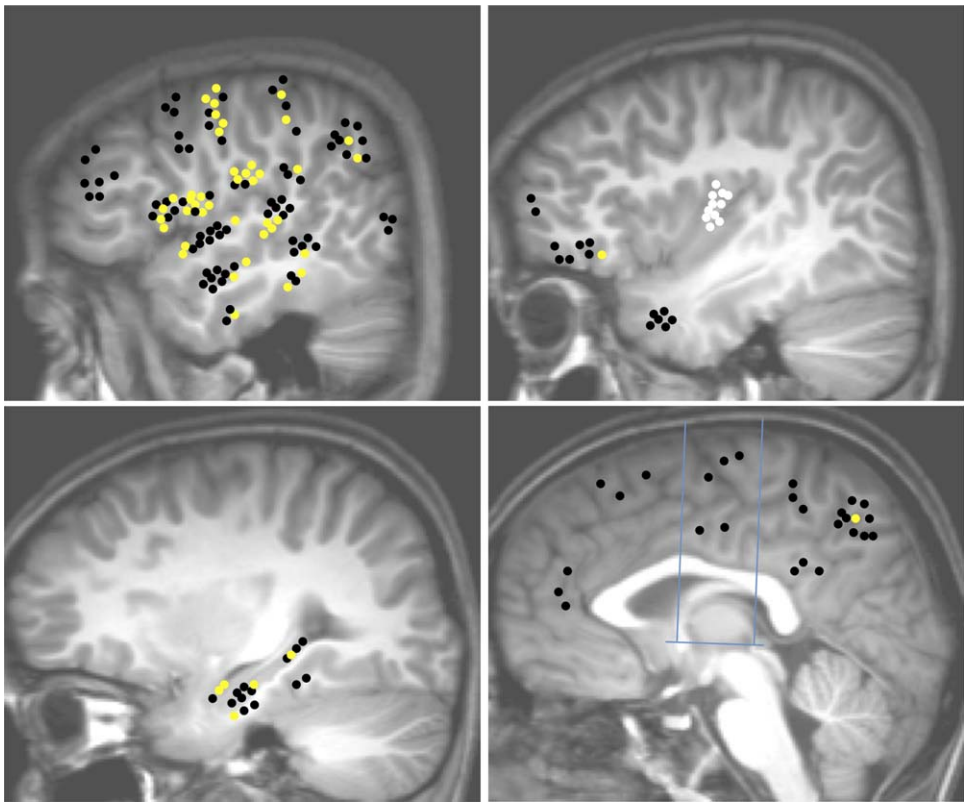

Figure 7.

ALG connectivity pattern: Upper left: Temporal neocortex, dorso-lateral frontal cortex, fronto-parietal operculum, temporo-parietal junction; Upper right: Insula, temporal pole, frontal pole and the fronto-orbital cortex; Lower left: mesio-temporal structures; Lower right: medial frontal, parietal and occipital cortices, cingulate gyrus. Blue lines in the lower right figure indicate CA-CP axis and the orthogonal VCA and VCP axis. Yellow dots: connections demonstrating significant CCEPs; Black dots: connections without significant CCEP; White dots: ALG electrodes.

with the regions responsible for emotional processing and cognitive control [Deen et al., 2011]. This view is supported by structural imaging studies which indicate that the cortical regions receiving most of the projections from the anterior insula constitute a ventrally based network including the orbitofrontal cortex, the frontal operculum, the temporal pole, and the amygdala [Cerliani et al., 2011], and forming part of a key emotional salience and cognitive control network associated with the implementation of goal-directed behavior [Cloutman et al., 2011]. For reasons explained above, our own findings regarding the anterior insula are limited to its dorsal and dysgranular part. Nevertheless, we could confirm ASG connectivity with the anterior fronto-temporal brain regions, including the temporal pole and orbitofrontal cortex, as well as with the hippocampus, in line with a previous CCEPs study of hippocampal connectivity performed by our group on a different set of patients [Catenoix et al., 2011]. However, this pattern was partly different for the MSG which had the lowest connectivity rate with nonopercular brain regions (i.e., 9% as compared to 36% for the ASG) and was not connected to the orbitofrontal cortex. Conversely we observed a few connections between the MSG and both the precentral cortex and the parietal operculum, not previously identified as efferent targets of the anterior insula. Furthermore, ASG showed the lowest connectivity rate with the perisylvian region (40%), as compared to all four other insular gyri (66%), in line with its lower rate of intra-insular connectivity [Almashaikhi et al., 2013]. Thus, all above findings are in favor of a subdivision of the dorsal anterior insula into two distinct functional components centered around the ASG and MSG, respectively. We failed to identify CCEPs in the anterior cingulate cortex, in contrast with the classic view that the anterior insula is connected with this structure with which it shares specialized neurons (von Economo neurons) thought to play a role in social awareness [Allman et al., 2005, 2010]. As previously mentioned, this might reflect our restricted sampling of the pregenual aspect of the anterior cingulate. It might also points to truly different insula to cingulate

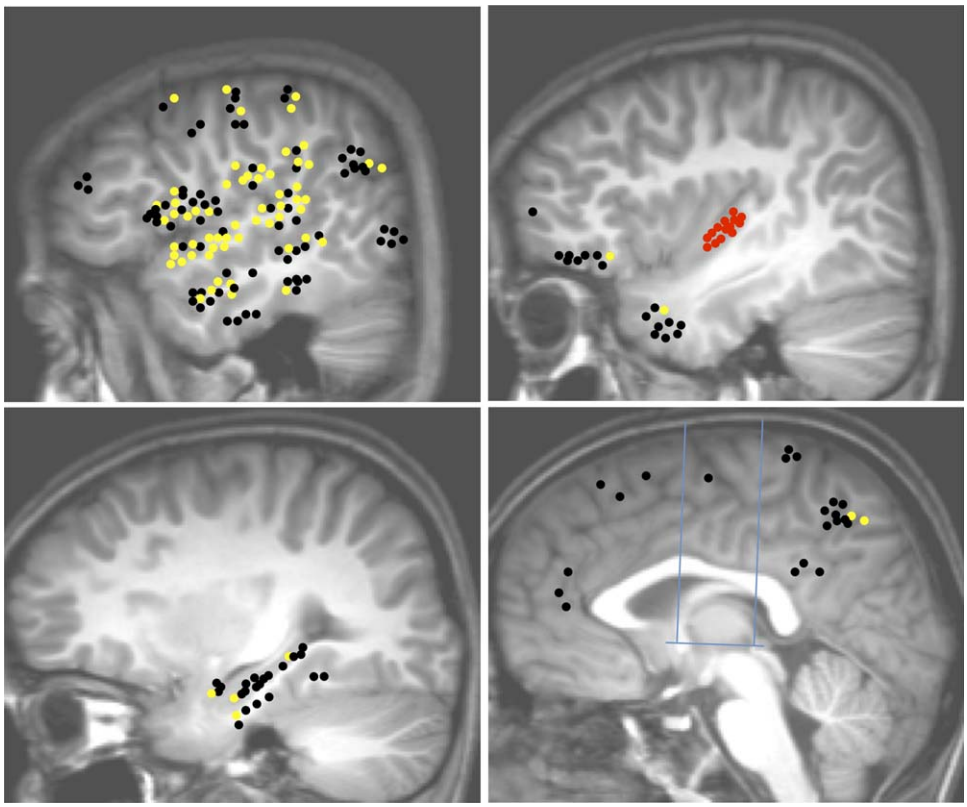

Figure 8.

PLG connectivity pattern: Upper left: Temporal neocortex, dorso-lateral frontal cortex, fronto-parietal operculum, temporo-parietal junction; Upper right: Insula, temporal pole, frontal pole and the fronto-orbital cortex; Lower left: mesio-temporal structures; Lower right: medial frontal, parietal and occipital cortices, cingulate gyrus. Blue lines in the lower right figure indicate CA-CP axis and the orthogonal VCA and VCP axis. Yellow dots: connections demonstrating significant CCEPs; Black dots: connections without significant CCEP; Red dots: PLG electrodes.

connectivity between macaque and human since several tractography studies also failed to detect connections between the ASG and the anterior cingulate cortex [Cerliani et al., 2011; Cloutman et al., 2011]. We also failed to detect connection between the anterior insula and both the amygdala and entorhinal cortex, but this finding remains unreliable according to the very small number of tested connections ($n = 3$).

The posterior insula, which usually includes the posterior short gyrus and dorsal aspect of the two long gyri, is connected with the orbitofrontal, mid and posterior cingulate, mesial and lateral premotor and somatosensory cortices, as well as with the temporal operculum and the amygdala in macaque [Mesulam and Mufson, 1982; Mufson and Mesulam, 1982; Mufson et al., 1981]. In human, the posterior insula was found to be functionally connected to primary and secondary motor and somatosensory cortices supporting its role in processing somatosensory stimuli with affective or motivational significance [Deen et al., 2011]. Tractography samples from the posterior dorsal insula reached the parietal lobe, the posterior part of temporal operculum, and extrastriate regions of the occipital cortex [Cerliani et al., 2011; Cloutman et al., 2011]. CCEPs obtained in our study partly confirmed these findings, by showing consistent connectivity of the posterior insula with the motor and sensory cortex, the parietal lobe (including the parietal operculum), and the temporal operculum, but also to a lesser degree with the frontal dorsolateral, orbitofrontal, lateral temporal and entorhinal cortices, the temporal pole and the hippocampus. Conversely, no connection was observed with the occipital lobe, mesial frontal cortex or mid and posterior cingulate gyri, a finding hampered by the small number of tested connections with each of these regions. Furthermore, some differences were observed between the different gyri constitutive of the posterior insula, with the PSG and PLG showing greater connectivity with the temporal operculum than the ALG (72% vs. 33%), while the PSG and ALG showed higher connectivity rates with the precentral cortex than the PLG (60% vs. 14%). Connectivity

rates with the frontal operculum also decreased from the PSG (71%) to the ALG (58%) and PLG (35%). The greater overall connectivity of the PSG is consistent with its higher rate of intra-insular connectivity [Almashaikhi et al., 2013], as well as its proposed role of a transitional and integrative area [Craig, 2010]. The reciprocity of CCEPs in the current study is slightly higher compared to other CCEP series performed on the motor system [Matsumoto et al., 2007], but consistent with anatomical data from rhesus monkeys where most of the insular connections were found to be reciprocal [Aggleton et al., 1980]. Insular efferences also demonstrated high degree of divergence with a median of four distinct brain regions showing CCEPs in response to individual insular stimulation, and 87% of insular bipoles being connected with at least two other brain structures. Such divergence has been described in other anatomical systems using CCEPs in human, in particular in the parietofrontal network [Matsumoto et al., 2012]. Both the high degree of reciprocity and divergence of the insular cortex connectivity appear in line with its complex integrative role in many sensory, cognitive and emotional functions [Kurth et al., 2010].

The morphology of CCEPs recorded in this series is comparable to that previously reported by our group and others in different brain regions [Catenoix et al., 2005, 2011; Lacruz et al., 2007; Matsumoto et al., 2004, 2007; Rosenberg et al., 2009]. Latencies of the first detectable peak were also consistent with the mean values found in previous studies, typically ranging between 20 and 30 ms [Matsumoto et al., 2004, 2007; Yamao et al., 2014]. However, we failed to demonstrate an association between the distance of the connections tested and their latency; in contrast with other series which have used subdural stimulation and recordings to study parieto-frontal networks for example [Matsumoto et al., 2012]. Reason for this discrepancy is unclear but might partially reflect differences in the intracranial electrodes used in both studies and related bias in the cortical structures sampled [i.e., unlike the depth electrodes used in our study, subdural grids as used in Matsumoto et al., 2012 will primarily sample the most superficial aspect of the cortical ribbon], and anatomical systems under study (i.e., insular efferences to any other lobe versus parieto-frontal network). This issue also points to the difficulties raised by the interpretation of CCEPs which latency, typically ≥ 20 ms, suggest polysynaptic responses [Catenoix et al., 2005].

We found limited connectivity between the insula and contralateral brain regions, specifically with the parietal operculum. This paucity of contralateral connections is in line with our previous observation of lack of inter-insular CCEPs in two patients who underwent bilateral implantation of the insula (patients #2 and 6 of this series) [Almashaikhi et al., 2013]. The interhemispheric connection observed in the present study might play a role in the sensorimotor function of the insula and also account for contralateral propagation of insular seizures.

Overall, electrically induced corticocortical EPs demonstrate that the human insula is characterized by rich reciprocal connections with several brain regions, most of which are in line with previously identified functional networks in macaques and neuroimaging studies in human. However, although differences were observed in the pattern of connectivity of the different subdivisions of the insula, a larger than previously reported redundancy was noted, consistent with the rich intra-insular connectivity recently reported [Almashaikhi et al., 2013]. From an epilepsy point of view, this suggests that propagation of insular seizures might be more diverse and complex than what has been suggested on the basis of a few observations [Ryvlin, 2006; Ryvlin et al., 2006b]. The main unexpected finding was the lack of detected connection between the insula and the cingulate gyrus as well as with the SMA and pre-SMA. This negative finding might just reflect the sample limitations of our series, justifying further studies in larger population.

REFERENCES

Afif A, Mertens P (2010b): Description of sulcal organization of the insular cortex. Surg Radiol Anat 32:491–498.

Afif A, Minotti L, Kahane P, Hoffmann D (2010a): Anatomofunctional organization of the insular cortex: A study using intracerebral electrical stimulation in epileptic patients. Epilepsia 51: 2305–2315.

Aggleton JP, Burton MJ, Passingham RE (1981): Cortical and subcortical afferents to the amygdale of the rhesus monkey (*Macaca mulatta*). Brain Res 190:347–368.

Aguera PE, Jerbi K, Caclin A, Bertrand O (2011): ELAN: A software package for analysis and visualization of MEG, EEG, and LFP signals. Comput Intell Neurosci 2011:158970.

Allman JM, Watson KK, Tetreault NA, Hakeem AY (2005): Intuition and autism: A possible role for Von Economo neurons. Trends Cogn Sci 9:367–373.

Allman JM, Tetreault NA, Hakeem AY, Manaye KF, Semendeferi K, Erwin JM, Park S, Goubert V, Hof PR (2010): The von Economo neurons in frontoinsular and anterior cingulate cortex in great apes and humans. Brain Struct Funct 214:495–517.

Almashaikhi T, Rheims S, Ostrowsky-Coste K, Montavont A, Jung J, De Bellescize J, Arzimanoglou A, Keo Kosal P, Guénot M, Bertrand O, Ryvlin P (2014): Intrainsular functional connectivity in human. Hum Brain Mapp 35:2779–2788.

Augustine JR (1996): Circuitry and functional aspects of the insular lobe in primates including humans. Brain Res Rev 22: 229–244.

Brazier MA (1964): Evoked responses recorded from the depths of the human brain. Ann N Y Acad Sci 112:33–59.

Buser P, Bancaud J (1983): Unilateral connections between amygdala and hippocampus in man. A study of epileptic patients with depth electrodes. Electroencephalogr Clin Neurophysiol 55:1–12.

Buser P, Bancaud J, Chauvel P (1992): Callosal transfer between mesial frontal areas in frontal lobe epilepsies. Adv Neurol 57: 589–s604.

Catenoix H, Magnin M, Guenot M, Isnard J, Mauguiere F, Ryvlin P (2005): Hippocampal-orbitofrontal connectivity in human: An electrical stimulation study. Clin Neurophysiol 116:1779–1784.

Catenoix H, Magnin M, Mauguiere F, Ryvlin P (2011): Evoked potential study of hippocampal efferent projections in the human brain. Clin Neurophysiol 122:2488–2497.

Cauda F, D'Agata F, Sacco K, Duca S, Geminiani G, Vercelli A (2011): Functional connectivity of the insula in the resting brain. Neuroimage 55:8–23.

Cerliani L, Thomas RM, Jbabdi S, Siero JC, Nanetti L, Crippa A, Gazzola V, D'Arceuil H, Keysers C (2011): Probabilistic tractography recovers a rostrocaudal trajectory of connectivity variability in the human insular cortex. Hum Brain Mapp 33: 2005–2034.

Cloutman LL, Binney RJ, Drakesmith M, Parker GJ, Ralph MA (2011): The variation of function across the human insula mirrors its patterns of structural connectivity: Evidence from in vivo probabilistic tractography. NeuroImage 59:3514–3521.

Craig AD (2010): The sentient self. Brain Struct Funct 214:563–577.

Deen B, Pitskel NB, Pelphrey KA (2011): Three systems of insular functional connectivity identified with cluster analysis. Cereb Cortex 21:1498–1506.

Gallay DS, Gallay MN, Jeanmonod D, Rouiller EM, Morel A (2011): The insula of Reil revisited: Multiarchitectonic organization in macaque monkeys. Cereb Cortex 22:175–190.

Gordon B, Lesser RP, Rance NE, Hart J Jr, Webber R, Uematsu S, Fisher RS (1990): Parameters for direct cortical electrical stimulation in the human: Histopathologic confirmation. Electroencephalogr Clin Neurophysiol 75:371–377.

Guenot M, Isnard J, Ryvlin P, Fischer C, Ostrowsky K, Mauguiere F, Sindou M (2001): Neurophysiological monitoring for epilepsy surgery: The Talairach SEEG method. Stereotactic Funct Neurosurg 77:29–32.

Jakab A, Molnar PP, Bogner P, Beres M, Berenyi EL (2011): Connectivity-based parcellation reveals interhemispheric differences in the insula. Brain Topogr 25:264–271.

Kahane P, Tassi L, Francionne S, Hoffmann D, Lo Russo G, Munari C (1993): Manifestations électrocliniques induites par la stimulation électrique intracérébrale par chocs dans les épilepsies temporales. Clin Neurophysiol 22:305–326.

Kahane P, Minotti L, Hoffmann D (2004): Invasive EEG in the definition of the seizure onset zone: depth electrodes. In: Rosenow F, Lüders HO, editor. Handbook of Clinical Neurophysiology, Vol. 3. Presurgical Assessment of the Epilepsies with Clinical Neurophysiology and Functional Imaging. Amsterdam: Elsevier BV. pp 109–133.

Kurth F, Zilles K, Fox PT, Laird AR, Eickhoff SB (2010): A link between the systems: Functional differentiation and integration within the human insula revealed by meta-analysis. Brain Struct Funct 214:519–534.

Lacruz ME, Garcia Seoane JJ, Valentin A, Selway R, Alarcon G (2007): Frontal and temporal functional connections of the living human brain. Eur J Neurosci 26:1357–1370.

Matsumoto R, Nair DR, LaPresto E, Najm I, Bingaman W, Shibasaki H, Luders HO (2004): Functional connectivity in the human language system: A cortico-cortical evoked potential study. Brain 127:2316–2330.

Matsumoto R, Nair DR, LaPresto E, Bingaman W, Shibasaki H, Luders HO (2007): Functional connectivity in human cortical motor system: A cortico-cortical evoked potential study. Brain 130:181–197.

Matsumoto R, Nair DR, Ikeda A, Fumuro T, Lapresto E, Mikuni N, Bigaman W, Miamoto S, Fukuyama H, Takahashi R, Najm I, Shibasaki H, Luders HO (2012): Parieto-frontal network in human studied by cortico-cortical evoked potential. Hum Brain Mapp 33:2856–2872.

Meador KJ, Hermann B (2010): How localized is localization-related epilepsy? Neurology 75:386–387.

Mesulam MM (1985): The insula of Reil in man and monkey: Architectonics, connectivity and function. Cereb Cortex 4:179–226.

Mesulam M, Mufson EJ (1982): Insula of the old world monkey. III: Efferent cortical output and comments on function. J Comp Neurol 212:38–52.

Mufson EJ, Mesulam MM (1982): Insula of the old world monkey. II: Afferent cortical input and comments on the claustrum. J Comp Neurol 212:23–37.

Mufson EJ, Mesulam MM, Pandya DN (1981): Insular interconnections with the amygdale in the rhesus monkey. Neuroscience 6:1231–1248.

Munari C, Kahane P, Tassi L, Francione S, Hoffmann D, Lo RG, Benabid AL (1993): Intracerebral low frequency electrical stimulation: A new tool for the definition of the "epileptogenic area." Acta Neurochirurg Suppl 58:181–185.

Nathan SS, Sinha SR, Gordon B, Lesser RP, Thakor NV (1993): Determination of current density distributions generated by electrical stimulation of the human cerebral cortex. Electroencephalogr Clin Neurophysiol 86:183–192.

Ostrowsky K, Isnard J, Ryvlin P, Guenot M, Fischer C, Mauguiere F (2000): Functional mapping of the insular cortex: Clinical implication in temporal lobe epilepsy. Epilepsia 41:681–686.

Ostrowsky K, Magnin M, Ryvlin P, Isnard J, Guenot M, Mauguière F (2002): Representation of pain and somatic sensation in the human insula: A study of responses to direct electrical cortical stimulation. Cereb Cortex 12:376–385.

Pugnaghi M, Meletti S, Castana L, Francione S, Nobili L, Mai R, Tassi L (2011): Features of somatosensory manifestations induced by intracranial electrical stimulations of the human insula. Clin Neurophysiol 122:2049–2058.

Rosenberg DS, Mauguiere F, Catenoix H, Faillenot I, Magnin M (2009): Reciprocal thalamocortical connectivity of the medial pulvinar: A depth stimulation and evoked potential study in human brain. Cereb Cortex 19:1462–1473.

Rutecki PA, Grossman RG, Armstrong D, Irish-Loewen S (1989): Electrophysiological connections between the hippocampus and entorhinal cortex in patients with complex partial seizures. J Neurosurg 70:667–675.

Ryvlin P (2006): Avoid falling into the depths of the insular trap. Epileptic Disord 8 (Suppl 2):37–56.

Ryvlin P, Kahane P (2005): The hidden causes of surgery-resistant temporal lobe epilepsy: Extratemporal or temporal plus? Curr Opin Neurol 18:125–127.

Ryvlin P, Rheims S, Risse G (2006a): Nocturnal frontal lobe epilepsy. Epilepsia 47 (Suppl 2):83–86.

Ryvlin P, Minotti L, Demarquay G, Hirsch E, Arzimanoglou A, Hoffman D, Guénot M, Picard F, Rheims S, Kahane P (2006b): Nocturnal hypermotor seizures, suggesting frontal lobe epilepsy, can originate in the insula. Epilepsia 47:755–765.

Stephani C, Fernandez-Baca Vaca G, Maciunas R, Koubeissi M, Luders HO (2011): Functional neuroanatomy of the insular lobe. Brain Struct Funct 216:137–149.

Talairach J, Bancaud J (1973): Stereotaxic approach to epilepsy. Methodology of anatomo-functional stereotaxic investigations. Prog Neurol Surg 5:297–354.

Valentin A, Anderson M, Alarcon G, Seoane JJ, Selway R, Binnie CD, Polkey CE (2002): Responses to single pulse electrical stimulation identify epileptogenesis in the human brain in vivo. Brain 125:1709–1718.

Valentin A, Alarcon G, Garcia-Seoane JJ, Lacruz ME, Nayak SD, Honavar M, Selway RP, Binnie CD, Polkey CE (2005a): Single-pulse electrical stimulation identifies epileptogenic frontal cortex in the human brain. Neurology 65:426–435.

Valentin A, Alarcon G, Honavar M, Garcia Seoane JJ, Selway RP, Polkey CE, Binnie CD (2005b): Single pulse electrical stimulation for identification of structural abnormalities and prediction of seizure outcome after epilepsy surgery: A prospective study. Lancet Neurol 4:718–726.

van't Klooster MA, Zijlmans M, Leijten FS, Ferrier CH, van Putten MJ, Huiskamp GJ (2011): Time–frequency analysis of single pulse electrical stimulation to assist delineation of epileptogenic cortex. Brain 134:2855–2866.

Wilson CL, Isokawa M, Babb TL, Crandall PH (1990): Functional connections in the human temporal lobe. Exp Brain Res 82: 279–292.

Yamao Y, Matsumoto R, Kunieda T, Arakawa Y, Kobayashi K, Usami K, Shibata S, Kikuchi T, Sawamoto N, Mikuni N, Ikeda A, Fukuyama H, Miyamoto S (2014). Intraoperative dorsal language network mapping by using single-pulse electrical stimulation. Hum Brain Mapp 2014 Feb 24. doi: 10.1002/hbm.22479. [Epub ahead of print].